Modeling the Influence of Restriction Policies and Perceived Risk due to COVID-19 on Daily Activity Scheduling

Cloe Cortes Balcells* Fabian Torres* Rico Krueger† Michel Bierlaire*

July 3, 2024

Report TRANSP-OR 240703
Transport and Mobility Laboratory
School of Architecture, Civil and Environmental Engineering
Ecole Polytechnique Fédérale de Lausanne
transp-or.epfl.ch

*École Polytechnique Fédérale de Lausanne (EPFL), School of Architecture, Civil and Environmental Engineering (ENAC), Transport and Mobility Laboratory, Switzerland, {cloe.cortes, fabian.torres, michel.bierlaire}@epfl.ch

†Department of Technology, Management and Economics, Technical University of Denmark (DTU), rickr@dtu.dk

Abstract

This study develops an Activity-Based Model (ABM) framework to provide a deeper understanding of how activity restriction policies and perceived risks influence human mobility and, consequently, disease transmission. We propose three main contributions: i) the Activity-Based Restriction Model (ABRM) systematically implements various activity restriction policies, such as closures, curfews, and distance-based limitations, ii) we introduce a dynamic programming algorithm to address computational intractability in large-scale scenarios, significantly reducing computation time, iii) we build a Risk Perception Latent Variable Model to simulate how perceived risks influence individual scheduling behavior. By embedding this model into the ABRM, we create the Activity-Based Risk Perception Restriction Model (ABR^{2}M), which captures the dynamic interplay between risk perception and activity scheduling given activity-restriction policies. This integrated approach provides a detailed evaluation of individual schedules, offering valuable insights for the development of informed transportation policies.

Keywords: interdisciplinary discipline, discrete choice model, activity-based modeling, non-pharmaceutical interventions, public health policy, behavioral adaptations.

1 Introduction

The global COVID-19 pandemic has deeply disrupted individual daily schedules through both government-imposed restrictions, such as lockdowns and curfews, and personal behavioural adjustments influenced by risk perceptions (Rosi et al., 2021; Lu et al., 2024; Alsharawy et al., 2021). Such changes have reshaped daily life patterns, directly impacting disease transmission dynamics. Incorporating these behavioural shifts into epidemiological models is a valuable step for developing more effective public health strategies to control disease spread.

The relationship between human mobility and disease transmission, particularly in the context of COVID-19, has been a focus of significant research, establishing a bridge between transportation science and epidemiology. Several studies (Hancean et al., 2021, Mazzoli et al., 2020, Palguta et al., 2022) have explored how human movement patterns influence the transmission dynamics of diseases. Also, Tuomisto et al., 2020, Kerr et al., 2020, Aleta et al., 2020, and Cortes Balcells et al., 2023 employ detailed mobility data to simulate virus propagation, aiding in the forecasting of outbreak scenarios and the assessment of control measures. Despite these advancements, existing models do not systematically address

how individuals adjust their behaviour in response to various epidemic control measures and changes in subjective risk perceptions. In particular, the following research question remains unasked:

> *How do we account for risk perception and epidemic control restrictions in the context of mobility-based epidemiological models?*

Within this context, this study proposes an Activity Based Model (ABM) able to account for modification of daily schedule due to perceived risk through an endogenous choice set formation approach. The ABM, building on the specification of the model developed by Pougala et al., 2022, presents the following capabilities:

(a) It includes restriction policies, such as activity closures, curfews, and distance-based limitations imposed by the authorities.

(b) It incorporates a perceived risk latent variable model to simulate how individuals adjust their activity schedules based on perceived risks associated with specific activities.

(c) It significantly reduces computational time, achieving the global optima in approximately three hours for large city scenarios, thereby making it feasible to model and simulate extensive urban populations for policy-making.

The structure of this paper is as follows: Section 2 reviews the relevant literature and highlights the main research gaps. Section 3 includes policies to providing the formulation of our Activity-Based Restriction Model (ABRM). Section 4 presents the Activity-Based Risk & Restriction aware Model (ABR^{2}M). Both ABRM and ABR^{2}M are tested and compared to the standard ABM in Section 5. Finally, Section 6 outlines the conclusions and future research directions.

2 Literature Review

2.1 State of the Art of ABMs in Epidemiology

ABMs have become essential tools for understanding and predicting individual behavior patterns. These models simulate daily activities based on individual preferences, constraints, and interactions with the environment. They offer a granular approach to modeling human behavior by considering the sequence and timing of activities, making them highly suitable for studying the impacts of public health interventions. Several studies have demonstrated the application of ABMs in the epidemiological context (Aleta et al., 2020, Tuomisto et al., 2020, Kerr

et al., 2020, Hancean et al., 2021, Palguta et al., 2022).

For instance, Hancean et al., 2021 examine the impact of human mobility networks on the global spread of COVID-19. Their study underscores the importance of interconnected mobility patterns in facilitating the rapid spread of infectious diseases. Similar conclusions are drawn by Palguta et al., 2022, who investigate how elections impact COVID-19 transmission dynamics using an ABM to simulate the effects of increased human interactions during election periods.

More interestingly, Aleta et al., 2020 propose an ABM to model the impact of testing, contact tracing, and household quarantine on COVID-19 transmission in the Boston metropolitan area. Similarly, Tuomisto et al., 2020 develop the REINA model to simulate various policy actions on epidemic outcomes in the Helsinki University Hospital region. However, both studies do not include the possibility of having activity restriction policies, or lack the possibility of having different policies such as partial closures, curfews, and distance-based limitations.
A solution to this gap is provided by the work of Covasim framework (Kerr et al., 2020). Covasim is an ABM that integrates detailed mobility data to evaluate different interventions' effectiveness. Despite the significant improvement, Covasim does not consider the computational challenges posed by large-scale implementations, nor does it account for changes in individual activity schedules based on risk perception.

Overall, the literature lacks of a single ABM capable of considering restrictions and individual risk perception.

2.2 State of the Art ABMs for different application

ABMs have evolved over the past fifty years as an advancement over traditional trip-based models, addressing the complexities of individual behaviour in travel demand forecasting. These models are based on the principle that mobility is driven by the need to perform daily activities (see Hagerstrand, 2005). Understanding individuals' activity scheduling provides insights into their mobility choices, thus predicting travel demand more accurately. The primary assumption of ABMs is that travel behavior is a consequence of the need to perform activities. By modeling these needs, ABMs offer a behaviorally realistic approach to forecasting travel demand. ABMs can be broadly categorized into two types: utility-based models and computational process models.

Utility-based models, such as those proposed by Adler and Ben-Akiva, 1979 and Bowman and Ben-Akiva, 2001, optimize individuals' schedules to maximize utility under budget and time constraints. These models use discrete choice econo-

metric methods and have evolved to include micro-simulations for greater accuracy in capturing individual schedules. Notable examples include the STARCHILD model (Recker et al., 1986) and TRANSIMS (Beckman et al., 2002), which utilize synthetic populations to plan multimodal trips. Advanced techniques, like genetic algorithms employed by Charypar and Nagel, 2005, further enhance the realism by considering activity type, transportation mode, and location simultaneously.

On the other hand, computational process models reject the notion of optimal decision-making, instead suggesting that individuals use context-dependent heuristics (Arentze and Timmermans, 2004). These models simulate behavior by programming agents to follow specific rules and react to their environment, ranging from simple responses to complex adaptive behaviors. Computational process models offer a flexible approach to capturing the dynamic and context-specific nature of travel behavior.

Particularly interesting work has been done by Pougala et al., 2022, using a new modeling approach for daily activity scheduling which integrates the different daily scheduling choice dimensions (activity participation, location, schedule, duration and transportation mode) into a single optimization problem. In details, given a set of activities $\mathscr{A}$, the ABM optimization problem[1] for each individual n is defined as:

$$\max_{\omega,Z,x,\tau} \quad U_0 + \sum_{a=0}^{A} Z_a^0(\chi_a + V_a^1 + V_a^2) + \sum_{a=0}^{A}\sum_{b=0}^{A} Z_{ab}\cdot\theta_t\cdot\omega_{ab} \tag{1}$$

subject to:

$$\sum_a\sum_b (Z_a^0\cdot x_a^2 + Z_{ab}\cdot\omega_{ab}) = 24 \tag{2}$$

$$\omega_{\text{dawn}} = \omega_{\text{dusk}} = 1 \tag{3}$$

$$x_a^2 \geq Z_a^0\cdot\tau_a^{\min} \qquad \forall a\in\mathscr{A} \tag{4}$$

$$x_a^2 \leq Z_a^0\cdot T \qquad \forall a\in\mathscr{A} \tag{5}$$

$$Z_{ab} + Z_{ba} \leq 1 \qquad \forall a,b\in\mathscr{A}, a\neq b \tag{6}$$

$$Z_{a,\text{dawn}} = Z_{\text{dusk},a} = 0 \qquad \forall a\in\mathscr{A} \tag{7}$$

$$\sum_a Z_{ab} = Z_b^0 \qquad \forall b\in\mathscr{A}, b\neq \text{dawn} \tag{8}$$

$$\sum_b Z_{ab} = Z_a^0 \qquad \forall a\in\mathscr{A}, a\neq \text{dusk} \tag{9}$$

$$(Z_{ab}-1)\cdot T \leq x_a^1 + x_a^2 + Z_{ab}\cdot\omega_{ab} - x_b^1 \qquad \forall a,b\in\mathscr{A}, a\neq b, \tag{10}$$

[1]The description of the variables and parameters can be found in Appendix A, in Table 10. Note that the dependence on n is implicit in all Equations (1)–(14) and has been omitted for simplification purposes. For a detailed description of the problem see Pougala et al., 2022.

$$(1-Z_{ab})\cdot T \geq x^1_a + x^2_a + Z_{ab}\cdot \omega_{ab} - x^1_b \qquad \forall a,b \in \mathscr{A}, a \neq b \qquad (11)$$

$$x^1_a \geq \chi^-_a \qquad \forall a \in \mathscr{A} \qquad (12)$$

$$x^1_a + x^2_a \leq \chi^+_a \qquad \forall a \in \mathscr{A} \qquad (13)$$

$$\sum_{a\in\mathscr{F}_a} Z^0_a \leq 1 \qquad \forall a \in \mathscr{A} \qquad (14)$$

where:

$$V^1_a = \theta^{\text{early}}_a \cdot \max(0, \kappa_a - x^1_a - \Delta^{\text{early}}_a) + \theta^{\text{late}}_a \cdot \max(0, x^1_a - \kappa_a - \Delta^{\text{late}}_a) \qquad (15)$$

$$V^2_a = \theta^{\text{short}}_a \cdot \max(0, \tau_a - x^2_a - \Delta^{\text{short}}_a) + \theta^{\text{long}}_a \cdot \max(0, x^2_a - \tau_a - \Delta^{\text{long}}_a) \qquad (16)$$

In this work, we proposed different modifications to Problem (1-16) to:

(a) consider restriction policies,

(b) include individual perceived risk,

(c) make the problem tractable for large population scenarios.

3 Influence of Restriction Policies on Daily Activity Scheduling

3.1 Integration of Restriction Policies in the ABM: ABRM

This section includes the individual responses to public health policies during pandemics in the initially proposed ABM. The restriction policies are considered by complementing Problem (1)-(16) with new constraints and a new term on the objective function, to obtain the ABRM.

3.1.1 Modeling elements

The ABRM is operated under four main inputs:

1. **Individual Characteristics** x^e_{kn}: This includes details about each individual, such as their personal identifier, city of residence, age, employment status, and the identifiers and coordinates for their home and workplace.

2. **Facility Characteristics** x^f_m: This includes information about each facility, such as its identifier, type (e.g., education, shop, or leisure), type identifier, and geographic coordinates.

3. **Restriction Policies**: Each policy p involves activating a set of parameters from the set $\mathscr{P}$. Each element in $\mathscr{P}$ is defined as a set of parameters $\phi_{\ell,a}$, which takes

the value 1 if restriction ℓ is activated for activity a, and 0 otherwise. $\phi_{\ell,a}$ is a vector where each element ℓ corresponds to a specific type of restriction as

$$\ell = \begin{cases} 1 & \text{if Closure restrictions,} \\ 2 & \text{if Time slot starting time restrictions,} \\ 3 & \text{if Time slot closing time restrictions,} \\ 4 & \text{if Peak hour restrictions,} \\ 5 & \text{if Travel time restrictions,} \\ 6 & \text{if Curfew restrictions.} \end{cases}$$

4. **Desired Duration and Start Time for Each Activity and Individual**: This specifies when and for how long each individual wishes to perform their activities. The parameters κ_{an} and τ_{an}, represent the desired starting time and duration of activity a, respectively.

3.1.2 Optimization Problem

The objective function (1) is updated incorporating the term $\varphi_{5,a}V^3_{ab}$, to limit the distance between two activities a and b in term of time of travel, resulting in the final form of the function as follows:

$$\max_{\omega,Z,x,\tau} \quad U_0 + \sum_{a=0}^{A} Z^0_a(\chi_a + V^1_a + V^2_a + \varphi_{5,a}V^3_{ab}) + \sum_{a=0}^{A}\sum_{b=0}^{A} Z_{ab}\cdot\theta_t\cdot\omega_{ab} \tag{17}$$

where V^3_{ab} is defined as:

$$V^3_{ab} = \theta_t\cdot\omega_{ab}, \tag{18}$$

This addition together with restriction (25) ensures that individuals traveling from activity a to activity b to have a travel time smaller or equal to the constant t^5_θ. Moreover, considering the set of activities $\mathscr{A}$ and the set of constraints $\mathscr{P}$, the new activity restrictions for the optimization problem for each individual n can be defined as follows:

$$\varphi_{1,a}Z^0_a = 0 \qquad \forall\varphi_{1,a}\in\mathscr{P}, a\in\mathscr{A} \tag{19}$$
$$\varphi_{2,a}x^1_a \geq \varphi_{2,a}t^1_\Theta \qquad \forall\varphi_{2,a}\in\mathscr{P}, a\in\mathscr{A} \tag{20}$$
$$\varphi_{3,a}(x^1_a + x^2_a) \geq \varphi_{3,a}t^2_\Theta \qquad \forall\varphi_{3,a}\in\mathscr{P}, a\in\mathscr{A} \tag{21}$$
$$\varphi_{4,a}(x^1_a + x^2_a) \leq \varphi_{4,a}(t^3_\Theta + 24*(1-Z_2)) \qquad \forall\varphi_{4,a}\in\mathscr{P}, a\in\mathscr{A} \tag{22}$$
$$\varphi_{4,a}x^1_a \geq \varphi_{4,a}(t^4_\Theta - 24*(1-Z_1)) \qquad \forall\varphi_{4,a}\in\mathscr{P}, a\in\mathscr{A} \tag{23}$$
$$\varphi_{4,a}(Z_1 + Z_2 - 1) \geq 0 \qquad \forall a\in\mathscr{A} \tag{24}$$
$$\varphi_{5,a}(Z_{ab}\cdot\omega_{ab}) \leq \varphi_{5,a}t^5_\Theta \qquad \forall\varphi_{5,a}\in\mathscr{P}, a\in\mathscr{A} \tag{25}$$
$$\varphi_{6,a}\tau_{dawn} \leq \varphi_{6,a}t^6_\Theta \qquad \forall a\in\mathscr{A} \tag{26}$$

$$\varphi_{6,a} x_{dusk} \geq \varphi_{6,a} t^{7}_{\Theta} \qquad \forall a \in \mathscr{A} \qquad (27)$$

These new convex constraints (19)-(27) reflect multiple interventions, such as closure of activities (19), starting-time restrictions (20), ending-time restrictions (21), closing peak-hours restrictions (22)-(24), travel-time restrictions (26) and the activation of the term $\varphi_{5,a} V^{3}_{ab}$ from the objective function (1), and finally, curfew restrictions (26)-(27).

The mixed integer programming optimisation problem (17), (2)-(27) is the core of the proposed ABRM. This problem allows for not only integrating the different daily scheduling choice dimensions into a single optimization problem but also include individual responses to restriction policies.

3.2 Dynamic Programming and Computational Complexity

Problem (2)-(27) is difficult to solve with commercial solvers (e.g., CPLEX) in a reasonable amount of time. Indeed, the problem of finding the optimal daily schedule of an individual in the population is a variant of the well-know Elementary Shortest Path problem with Resource Constraints (ESSPRC) (see, Desaulniers et al., 2005), which is a common sub-problem for the solution of vehicle routing problems. The method used to solve this variant of the shortest path problem is usually a Dynamic Programming (DP) method, also known as labeling algorithms (e.g., Torres et al., 2022a, Torres et al., 2022b). In this work, we proposed a tailored DP algorithm to efficiently solve the ABRM problem. The rationale of the proposed DP algorithm is as follows:

- We use discretized time intervals of 5 minutes (i.e. 288 per day).
- We define a state using a label $\mathscr{L} = (a, U, t, x^{3}_{a}, u, \mathscr{R})$, where a is the current activity, U is the total utility collected including the current activity, t is the time interval, x^{3}_{a} is the duration of the activity, u is the cumulative cost, and $\mathscr{R}$ is the set of activities that cannot be reached[2].
- The algorithm starts with an initial label that represents the start of the day.
- At each iteration, the algorithm explores all possible feasible activities from the current state and extends the label to each activity[3].

Naturally, this method would lead to an exponential number of labels since we are expanding and creating labels for each possible feasible combination of activities and time. However, special techniques such as dominance rules are used to dominate a label, and thus, delete them, reducing significantly the number of labels necessary to reach the optimal solution. More details can be found in Appendix B.

[2]Activities can be unreachable either because they have been completed or they are mutually exclusive with completed activities.

[3]To extend a label $\mathscr{L}_k$ to a new activity a_j, we first check if the extension is feasible, ensuring that no constraints (such as time or budget) are violated and a_j is not in $\mathscr{R}_j$. If feasible, we create a new label $\mathscr{L}_j$ with updated resource states.

4 Influence of Perceived Risk due to COVID-19 on Daily Activity Scheduling

In this section, we investigate the inclusion of perceived risk in our model by examining its impact on individuals' scheduling choices. To achieve this, we first propose a method to estimate perceived risk as a latent variable model. We then assess its effect within a scheduling choice model. Based on the results, we determine the need to integrate this variable into the previously established ABM.

4.1 Perceived Risk Latent Variable Model

Employing a dataset that includes both attitudinal and explanatory variables, we propose to estimate a latent variable model to capture individuals' perceived risk of COVID-19. This model consists of a structural equation for the latent variable and a set of measurement equations that link this latent variable to observable indicators. The aim is to assess the risk perception levels (high, moderate, low) for various activities, such as work, leisure, and education, for each individual, based on their socioeconomic characteristics.

Structural Equation for the Latent Variable The latent variable for each individual, denoted as X_n^*, represents the high perceived risk and is estimated by the following structural equation:

$$X_n^* = \beta_0^* + \sum_{k=1}^{K} \beta_k^* x_{kn}^* + \sigma\epsilon^* \tag{28}$$

where: i) β_0^* is the intercept, ii) β_k^* are the coefficients for the K explanatory variables x_{kn}^* for each individual n, iii) σ is the standard deviation of the error term, iv) ϵ^* represents the error term associated with the latent variable..

Measurement Equations The indicators, measured on a Likert scale from 1 to 5, indicate risk perception or attitude toward COVID-19 by an individual n. These indicators are associated with the latent variable through the following measurement equations:

$$Y_{in}^* = \alpha_{0i}^* + \alpha_i^* X_n^* + \sigma_i^* \xi_i^* \tag{29}$$

where: i) α_{0i}^* is the intercept for the i-th indicator, ii) α_i^* is the coefficient relating the latent variable to the i-th indicator, iii) σ_i^* is the standard deviation of the error term for the i-th indicator, iv) ξ_i^* is the error term for the i-th indicator, v) τ_i are the thresholds that define the categories of the Likert scale.

$$Y_{in} = \begin{cases} 1 & \text{if } Y_{in}^* < \tau_1, \\ 2 & \text{if } \tau_1 \leq Y_{in}^* < \tau_2, \\ 3 & \text{if } \tau_2 \leq Y_{in}^* < \tau_3, \\ 4 & \text{if } \tau_3 \leq Y_{in}^* < \tau_4, \\ 5 & \text{if } \tau_4 \leq Y_{in}^*. \end{cases} \tag{30}$$

As the measurements are using a Likert scale with $M = 5$ levels, we define 4 parameters τ_i. The thresholds τ_i are defined symmetrically around zero to facilitate interpretation. For this reason, we define two positive parameters δ_1^* and δ_2^* as:

$$\begin{aligned}\tau_1 &= -\delta_1^* - \delta_2^*,\\ \tau_2 &= -\delta_1^*,\\ \tau_3 &= \delta_1^*,\\ \tau_4 &= \delta_1^* + \delta_2^*.\end{aligned}$$

Finally, the contribution to the likelihood for the ordered probit model is given by:

$$\begin{aligned}\Pr(Y_{in} = j_i) &= \Pr(\tau_{i-1} \leq Y_n^* \leq \tau_i)\\ &= \Pr\left(\frac{\tau_{i-1} - \alpha_{0i}^* - \alpha_i^* X_n^*}{\sigma_i^*} < \xi_i \leq \frac{\tau_i - \alpha_{0i}^* - \alpha_i^* X_n^*}{\sigma_i^*}\right)\\ &= \Phi\left(\frac{\tau_i - \alpha_{0i}^* - \alpha_i^* X_n^*}{\sigma_i^*}\right) - \Phi\left(\frac{\tau_{i-1} - \alpha_{0i}^* - \alpha_i^* X_n^*}{\sigma_i^*}\right).\end{aligned} \tag{31}$$

where Φ denotes the cumulative distribution function of the standard normal distribution.

4.2 Assessing the Impact of Perceived Risk on Scheduling Choices

To understand if perceived risk is changing individual choices, we begin by estimating its impact in a simple binary choice model. This model presents the alternative between two mutually exclusive activities, for instance working from home or working from the office. This approach helps us establish the role of risk perception in scheduling decision-making. Although this is a simplification to study the impact of perceived risk, it can be extended to more complex scenarios.

Latent variables can be included in choice models. Consider a binary choice model with two alternatives. The utility functions are of the following form:

$$\begin{aligned}U_1 &= 0,\\ U_2 &= V_2 + \varepsilon_2 = \mathrm{ASC}_2 + \beta_2^{\mathrm{T}}\ \mathrm{Time}_{\,2} + \varepsilon_2\end{aligned} \tag{32}$$

where Time_2 is the travel time to go to alternative 2, and β_2^{T} is defined as:

$$\beta_2^{\mathrm{T}} = \beta_2^{'\mathrm{T}} \exp(-\beta_2^{X^\star} X^\star), \tag{33}$$

where $X^\star$ is defined by (28), so that

$$\beta_2^{\mathrm{T}} = \beta_2^{'\mathrm{T}} \exp\left(-\beta_2^{X^\star}\left(\bar{X}^s + \sigma\epsilon^*\right)\right). \tag{34}$$

Technically, such a choice model can be estimated using the choice observations only, without the indicators. Assuming that ε_2 is i.i.d. extreme value distributed, we have

$$\begin{aligned}\Pr(2 \mid \epsilon^*) &= \frac{\exp(\mathbf{V}_2)}{\exp(V_2) + \exp(V_1)}\\ \Pr(2) &= \int_{\epsilon^*=-\infty}^{\infty} \Pr(2 \mid \epsilon^*)\phi(\epsilon^*)d\epsilon^*,\end{aligned}$$

where $\phi(\cdot)$ is the probability density function of the univariate standardized normal distribution. The choice model is a mixture of logit models.

After estimating the parameters, if both parameters $\beta_2^{X^\star}$ and $\beta_2^{'T}$ are significant, we expect $\beta_2^{'T}$ to be positive, since it represents a positive effect on utility from travel time.This would mean that risk awareness has a significant impact and needs to be considered in scheduling choices.

To further study impact of the latent variable in the choice of the alternative, we compute the marginal utility of $\beta_2^{X^\star}$. Specifically:

$$\frac{\partial U_2}{\partial \beta_2^{X^\star}} = -(\beta_2^{'T} X^\star)\text{Time}_2 \exp(-\beta_2^{X^\star} X^\star). \tag{35}$$

Since $\exp(-\beta_2^{X^\star} X^\star)$ is always positive regardless of the values of $\beta_2^{X^\star}$ and $X^\star$, the sign of $\frac{\partial U_2}{\partial \beta_2^{X^\star}}$ is determined by $-\beta_2^{'T} X^\star \text{Time}_2$:

- If $\beta_2^{'T} > 0$ and $X^\star > 0$, the derivative is negative.
- If $\beta_2^{'T} > 0$ and $X^\star < 0$, the derivative is positive.
- If $\beta_2^{'T} < 0$ and $X^\star > 0$, the derivative is positive.
- If $\beta_2^{'T} < 0$ and $X^\star < 0$, the derivative is negative.

Now, we can compute the probabilities of each alternative. In order to include the impact of the perceived risk of the non-selected alternative in our scheduling problem, we can modify the desired duration τ_a. By setting the desired duration of the non-picked activity to zero in the ABRM model, it ensures that the non-selected activity is not included in the individual's schedule, effectively modifying their schedule based on the perceived risk.

5 Case Studies and Performance Assessment

In this section, we validate and demonstrate the operation of both ABRM and ABR^{2}M. Section 5.1 illustrates how various policies impact mobility patterns, while Section 5.2 explores how perceived risk modifies individual schedules. These case studies provide valuable insights into the effectiveness and adaptability of our models in real-world scenarios.

5.1 Restriction Policies Influence on Daily Activity Scheduling

5.1.1 Data

As input for the ABRM model, we need to provide a synthetic population that includes individual-level demographic and socio-economic characteristics, as well as a network outlining the spatial layout of activities. In this case, we use the open-source synthetic

population provided by He et al., 2020 for a sample of of 320,000 individuals and 207,370 facilities, which includes data on individuals' age, gender, employment status, and education level. Additionally, this synthetic dataset integrates a geographic network that assigns coordinates to nodes, each tagged with specific activity types such as education, work, secondary, and home. Finally, we use the desired schedules for each individual provided by this data-frame to derive distributions on desired start time and duration for each activity. This distributions are computed conditional to age and employment. As socio-demographic information of the individuals, we include the attributes of age, gender, employment status, and education level. As facility information, we incorporate the type of facility (e.g., education, shop, home, or secondary), and their geographic coordinates. The desired duration τ_{an} and start time κ_{an} for each individual are drawn from distributions based on the binary variable of employment status, and four age categories: child (0-18), young adult (18-30), adult (30-60), and elder (60+). As policy inputs, we explore seven different scenarios p, each representing a different imposed policy p, as detailed in Table 1. Note that if a combination of restriction $\varphi_{\ell,a}$ is not activated, it is set to 0. Table 1 presents the different tested scenarios, each considering various restriction

Tested Scenarios	**Closure**			**Constraints**
	Secondary	Education	Work	Curfew
No restrictions				
Outing limitations	$\varphi_{1,\text{secondary}} = 1$			
Early curfew	$\varphi_{6,\text{secondary}} = 1$	$\varphi_{6,\text{education}} = 1$	$\varphi_{6,\text{work}} = 1$	$t_{\Theta}^{7} = 5\text{pm}$
Economy preservation	$\varphi_{1,\text{secondary}} = 1$	$\varphi_{1,\text{education}} = 1$		
Work-education balance		$\varphi_{1,\text{education}} = 1$	$\varphi_{1,\text{work}} = 1$	
Secondary facilities closure	$\varphi_{1,\text{secondary}} = 1$			

Table 1: Tested scenarios, each one considering different NPIs as input to the ABM.

policies input to the ABRM. In particular:

- **No restrictions**: Represents a baseline with no imposed restrictions.
- **Outing limitations**: Activates constraint $\varphi_{1,\text{secondary}} = 1$ in Eq. (19) for the secondary activities, closing fully these activities.
- **Early curfew**: Activates constraints $\varphi_{6,\text{secondary}} = 1$, $\varphi_{6,\text{education}} = 1$, and $\varphi_{6,\text{work}} = 1$ in Eq. (26) and (27). The curfew constraint $t_{\Theta}^{7} = 5\text{pm}$ limits activities after dusk.
- **Economy preservation**: Activates constraints $\varphi_{1,\text{secondary}} = 1$ and $\varphi_{1,\text{education}} = 1$ in Eq. (19), but preserves economic activities.
- **Work-education balance**: Activates constraints $\varphi_{1,\text{education}} = 1$ and $\varphi_{1,\text{work}} = 1$ in Eq. (19), balancing restrictions between work and education activities.

- **Secondary facilities closure**: Activates constraint $\varphi_{1,\text{secondary}} = 1$ in Eq. (19), targeting the closure of secondary facilities.

These constraints enforce different combinations of activity restrictions, representing various policy measures to control mobility and activity patterns.

5.1.2 Aggregated Validation of Activity Patterns Throughout Scenarios

Figure 1 displays the total number of individuals engaged in each activity type across different intervention scenarios throughout the day and allows for assessing whether the simulated activity patterns align with the restrictions we have imposed. The *'Normal*

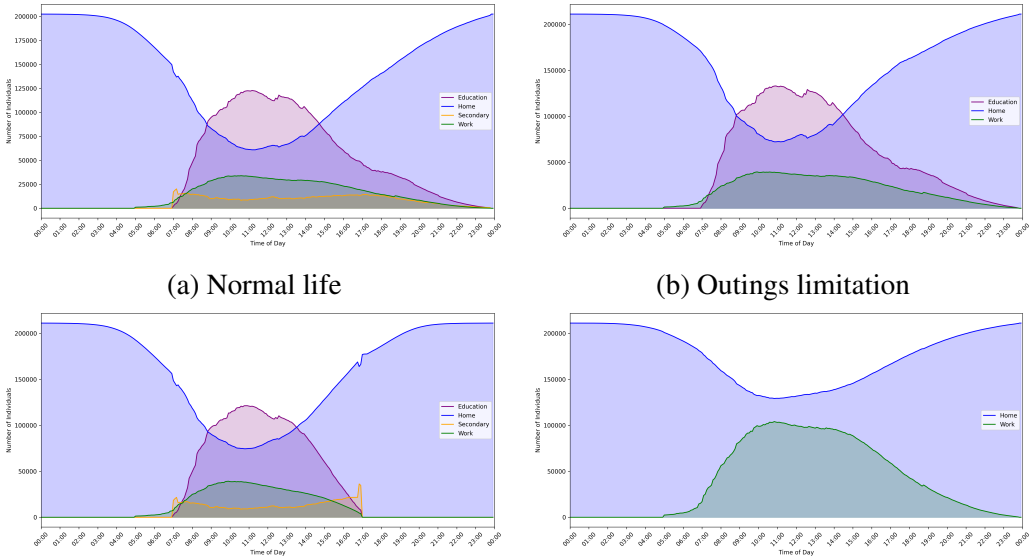

(a) Normal life

(b) Outings limitation

(c) Early curfew

(d) Only economy

Figure 1: Aggregated visualization of the total count of individuals in each activity throughout the day under various scenarios. Activities are represented as follows: Home (blue), Education (purple), Work (green), and Secondary (orange).

Life' scenario (Fig. 1a) provides a baseline for comparison, depicting a typical day without restrictions. In the *'Outings Limitation'* scenario, visible in Fig. 1b, we observe that all secondary activities disappear. Additionally, there is an increase in work activities, as work becomes the only allowed activity. In contrast, the *'Early Curfew'* scenario (Fig. 1c) reveals a significant decline in evening activities, reflecting adherence to the imposed 5 PM curfew. The model effectively reschedules activities earlier in the day to comply with the curfew restrictions. Interestingly, there is a noticeable delay between the time activities conclude and the time individuals return home, due to the travel time from the last activity to their residence. Finally, the *'Only Economy'* scenario (Fig. 1d) shows the closing of secondary and educational activities.

Overall, the changes across all scenarios align with the constraints imposed in the simulation, showing that the ABRM can accurately model the imposed restrictions through noticeable changes in activity patterns, validating the model's sensitivity to different restriction policies. This validation is crucial for ensuring the model's reliability in predicting how different policies can influence public behavior and mobility, thereby aiding in the design and implementation of effective transportation and public health interventions.

5.1.3 Disaggregated Consistency Check of the Baseline Scenario

Table 2 examines the schedules of randomly picked individuals in the baseline scenario, to check whether the simulation captures the variability inherent in real-world behaviour. The table displays the schedule of Individual 2837 (6-year-old kid), Individual 2107 (20-year-old partially employed student), and Individual 0107 (47-year-old employed adult). The schedule differences show that the model accurately reflects individual variations in activity patterns, which is critical for the realistic simulation of disease spread. Although this is not a model validation, it is an important consistency check for the baseline scenario, showcasing the ability of the model to capture such detail at the individual level, making it suitable for further epidemiological analysis.

Time	**Individual n.2837** (6-year-old)	**Individual n.2107** (20-year-old)	**Individual n.0107** (47-year-old)
00:00 - 07:00	Home	Home	Home
07:00 - 08:00	Home	Home	Home
08:00 - 09:00	School	Home	Work
09:00 - 13:00	School	University	Work
13:00 - 15:00	Home	Secondary	Work
15:00 - 18:00	Home	Work	Home
18:00 - 24:00	Home	Home	Home

Table 2: Hourly Daily Schedule of Individuals

5.1.4 Behavioral Adaptations

One of the most significant features of the proposed framework is that it allows individuals to adjust their schedules in response to the introduction of restriction policy. This capability reveals diverse individual and population-level responses to various mobility restriction scenarios. To provide an overview of these rescheduling choices, we present Figure 2, which illustrates the activity-swapping phenomenon. By examining the total duration per activity type, we observe that if secondary and education facilities are closed (as in the *'Only Economy'* scenario), individuals increase the time spent at work since it remains the only permissible activity outside the home. This activity-swapping mechanism is evident across all scenarios. When observing the histogram of total duration per

activity type for different policies p, it is apparent that the total duration for each activity type always differs compared to the *'Normal Life'* scenario. If this were not the case, activities would either be closed or remain unchanged, and the excess individuals unable to perform the closed activities would shift to spending more time at home. Note that these results are derived from the ABRM framework, which does not include risk perception in the activity scheduling process. If rescheduling is not modeled within the ABRM framework, and activities are simply set to zero when closed (e.g., closing work and setting work to zero), it overlooks the fact that individuals will reallocate their time to other activities. Thus, it is crucial for policy-making to account for rescheduling to accurately predict how people adapt to restrictions since it directly impacts on how and when people meet, and therefore the spread of the disease.

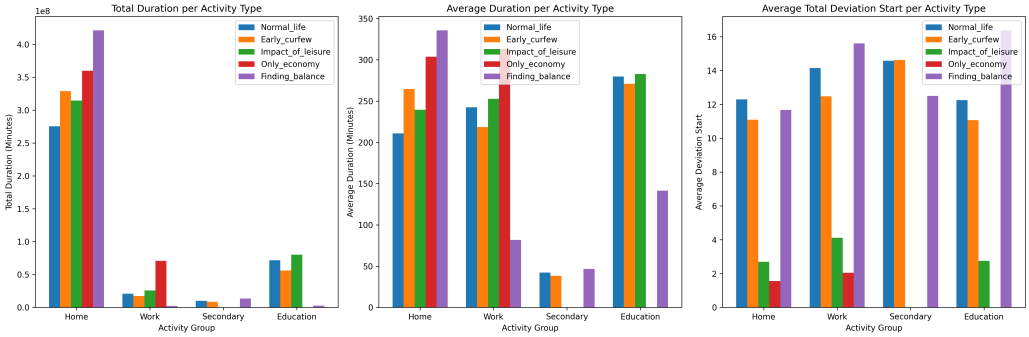

Figure 2: Total Duration, Average Duration and Average Total Deviation Start per Activity Type.

5.1.5 Tested Scenarios and Computational Complexity

The model efficiently manages a facility choice set of 207,370 with a population of 320,000, achieving an average execution time of 3h and 12 minutes for the *'No Restriction'* scenario, as detailed in Table 3. The significantly reduced runtime of 5 minutes for the *'Economy Preservation'* scenario is due to the decreased choice set of facilities, as only work activities are available, and only employed adults need to schedule activities while the rest of the population stays home. These results show the model's computational robustness for 1000 draws. A similar concept can be applied to explain the differences in runtime for the other scenarios, where the restrictions on activities and population segments lead to variations in computational complexity. Our method significantly outpaces the model created by Pougala et al., 2022 in terms of speed. Using their model for a choice set as large as 207,370 would not be feasible, underscoring the difficulties of efficiency and scalability when dealing with larger groups and more extensive sets of facilities.

5.1.6 Discussion

To conclude, the main takeaways of this first study case are here below summarised:

	Execution time [h:mm:ss]	individuals/second	seconds/individual
No restrictions	3:12:42	16.57	0.06
Outing limitations	0:45:24	69.01	0.014
Early curfew	3:05:54	16.85	0.059
Economy preservation	0:05:29	570.13	0.0018
Work-education balance	2:26:55	21.33	0.047
Leisure facilities closure	1:12:51	43:01	0.023

Table 3: Execution details, for each tested scenario.

- **Section 5.1.2**: The ABRM model accurately captures the impact of various restriction policies on activity patterns, validating its sensitivity to policy changes.
- **Section 5.1.3**: The model accurately reflects diverse daily routines of different demographic groups, ensuring robustness in simulating real-world behaviors.
- **Section 5.1.4**: The model simulates behavioral adaptations, showing individuals adjust schedules under different restriction policies, demonstrating its dynamic nature.
- **Section 5.1.5**: The model is computationally efficient, handling large populations and complex scenarios effectively, with execution times varying based on restriction levels.

5.2 Perceived Risk Influence on Daily Activity Scheduling

5.2.1 Data

This study uses a survey dataset (see Chauhan et al., 2022) collected in the US during the COVID-19 pandemic to analyze the impacts on individuals' mobility patterns and travel decisions. The survey was conducted in three waves: the first from April 2020 to June 2021, the second from November 2020 to August 2021, and the third from October 2021 to November 2021. In total, 9,265 responses were collected initially, with 2,877 participants returning for the second wave and 2,728 for the third. This dataset allows for the calibration of the latent variable model which integrates behavioural responses to COVID-19. The survey dataset includes responses from a diverse demographic, providing detailed information on their mobility patterns, including the frequency of performing an activity a during the pandemic. Specifically, the survey collected data on pre-pandemic commute times, specifically asking participants:

> "Before the COVID-19 pandemic, how many minutes did it usually take you to get to work?"

The responses regarding pre-pandemic commute times were categorized into nine travel time bins, as follows:

$$\text{Time}_{\text{WFO}} = \begin{cases} < 48\text{m} & & \\ \geq 48\text{m} & \& & < 96\text{m} \\ \geq 96\text{m} & \& & < 144\text{m} \\ \geq 144\text{m} & \& & < 192\text{m} \\ \geq 192\text{m} & \& & < 240\text{m} \\ \geq 240\text{m} & \& & < 288\text{m} \\ \geq 288\text{m} & \& & < 336\text{m} \\ \geq 336\text{m} & \& & < 384\text{m} \\ \geq 432\text{m} & \& & < 480\text{m} \end{cases}$$

where WFO is Work From Office. Additionally, we observe i attitudinal variables for each individual n, noted as Y_{in}. Y_{in} reflects the individuals' risk perceptions and concerns regarding the pandemic. These responses are key in modeling the psychological underpinnings influencing activity-travel behavior during a public health crisis. The list of indicators can be found in Table 4. The survey also includes the socio-demographic information of the respondents[4].

5.2.2 Latent Variable Model Results

In our study, we employed Exploratory Factor Analysis (EFA) to investigate the underlying structure of the attitudinal dataset, aiming to identify latent factors that capture the correlations among observed variables related to individuals' travel behaviors during the COVID-19 pandemic. From this, we keep the indicators belonging to Factor 1, that describe our latent variable named High_Risk_Perceived. The progression from a simple model to one with additional indicators and variables is done systematically, with each step evaluated for improved likelihood and significance of parameters.[5]

The final model of X_n^* presented in Eqs. (28) and (29) includes 4 different explanatory variables x_{nk}^e (gender, ethnicity, educational level and location), 8 indicators Y_{in} (risk_percp_1, risk_percp_2, risk_percp_3, risk_percp_5, risk_percp_6, att_covid_friends severe, att_covid_stayhome,att_covid_sh_norm) and is shown in Figure 3. The demographic coefficients β_k^* of the explanatory variables are visible in Table 5 and explain the difference in how various groups perceive risk. In particular, negative coefficients indicating a lower perceived risk among females, non-Caucasian and people with low education respondents compared to their counterparts. Meanwhile, regional differences are also evident, as seen in the negative coefficient for respondents living in the Western region, possibly hinting at regional variations in COVID-19 impact or public health responses.

[4]Each Information k of the individual n is represented as x_{kn} in the dataset visible in Table 7.

[5]Table 8 quantitatively interprets how respondents' perceptions of COVID-19 risk across various everyday activities relate to the latent variable 'High_Risk_Perceived'.

Name	Description	N	Histogram of Responses
att_covid_selfsevere	If I catch the coronavirus, I am concerned that I will have a severe reaction.	1716	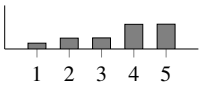
att_covid_friendssevere	I am concerned that friends or family members will have a severe reaction to the coronavirus if they catch it.	1716	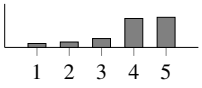
att_covid_stayhome	Everyone should just stay home as much as possible until the coronavirus has subsided.	1716	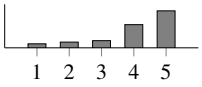
att_covid_overreact	Society is overreacting to the coronavirus.	1716	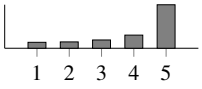
att_covid_economic	Shutting down businesses to prevent the spread of coronavirus is not worth the economic damage that will result.	1716	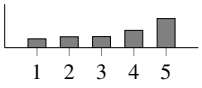
att_covid_sh_norm	My friends and family expect me to stay at home until the coronavirus subsides.	1716	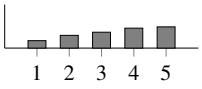
att_covid_mask	Everyone should wear a mask when in public indoor spaces.	1716	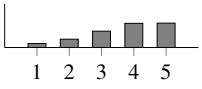
risk_percp_1	How do you perceive your COVID-19 risk from going to work?	900	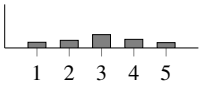
risk_percp_2	How do you perceive your COVID-19 risk from shopping at a grocery store?	1716	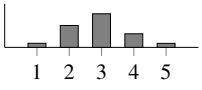
risk_percp_3	How do you perceive your COVID-19 risk from riding public transportation?	1715	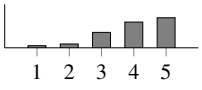
risk_percp_4	How do you perceive your COVID-19 risk from walking or bicycling?	1716	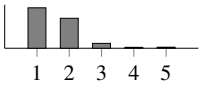
risk_percp_5	How do you perceive your COVID-19 risk from taking a taxi or ride-hailing service?	1716	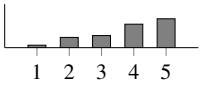
risk_percp_6	How do you perceive your COVID-19 risk from traveling in an airplane?	1716	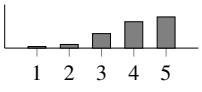

Table 4: COVID-19 Attitudes and Risk Perception Indicators. Coding for agreeing indicators: 1=Strongly disagree, 2=Somewhat disagree, 3=Neutral, 4=Somewhat agree, 5=Strongly agree, -1= Question not displayed to respondent. Coding for risk indicators: 1=Extremely low risk, 2= Low risk, 3=Medium risk, 4=High risk, 5=Extremely high risk.

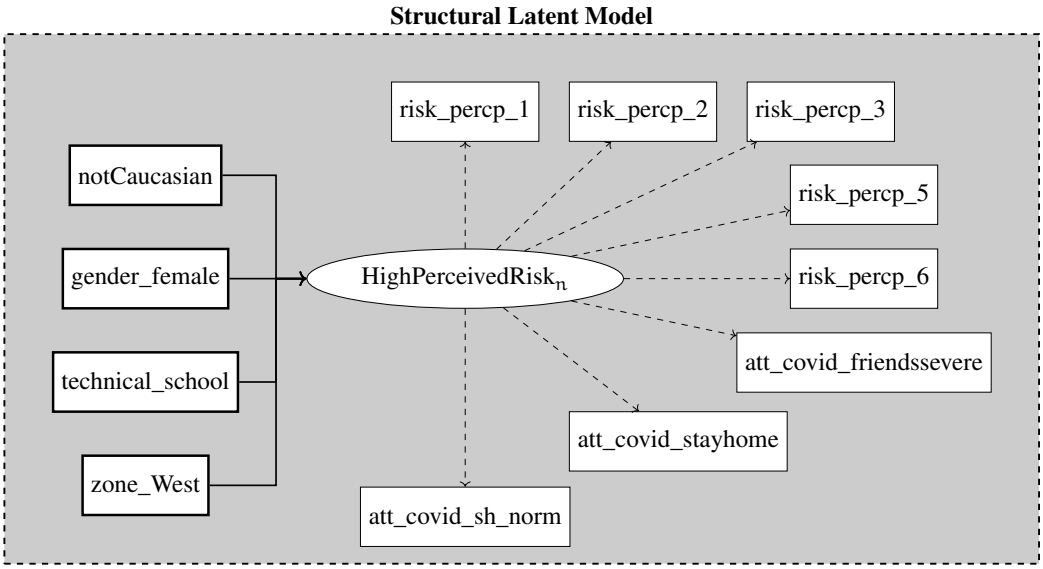

Figure 3: Diagram of the Risk Perception Latent Variable Model

β_k^*	**Value**	**Rob. Std err**	**Rob. t-test**	**Rob. p-value**
$\beta^\star$_gender_female	-0.25	0.0478	-5.23	1.67×10^{-7}
$\beta^\star$_notCaucasian	-0.265	0.0509	-5.2	1.94×10^{-7}
$\beta^\star$_technical_school	0.142	0.0583	2.44	1.47×10^{-2}
$\beta^\star$_zone_West	0.0905	0.0421	2.15	3.16×10^{-2}
α_i^*	**Value**	**Rob. Std err**	**Rob. t-test**	**Rob. p-value**
$\alpha^\star$_risk_percp_1	0.64	0.127	5.04	4.54×10^{-7}
$\alpha^\star$_risk_percp_2	0.376	0.0878	4.28	1.86×10^{-5}
$\alpha^\star$_risk_percp_3	0.372	0.0874	4.26	2.08×10^{-5}
$\alpha^\star$_risk_percp_5	0.273	0.0792	3.45	5.62×10^{-4}
$\alpha^\star$_risk_percp_6	0.406	0.0891	4.55	5.27×10^{-6}

Table 5: Selected results parameters from Latent model

Moving to the measurement equations, the parameters α_i^*, also visible in Table 5, reflect respondents' perceived risk from engaging in specific activities: shopping at a grocery store, riding public transportation, and using a taxi or ride-hailing service, etc. The positive values of these parameters indicate a direct correlation - those who perceive greater risks associated with these activities contribute to a higher perceived risk. For instance, $\alpha^\star$_risk_percp_2's positive coefficient suggests that individuals who perceive a higher risk from shopping at grocery stores also tend to report a higher overall perceived risk of COVID-19. This is intuitive as grocery shopping involves being in relatively enclosed spaces with other people, a condition that could increase the perceived risk of virus transmission. Similarly, $\alpha^\star$_risk_percp_3's significance reflects concerns over the close quarters and high contact nature of public transportation, while the positive coefficient for

$\alpha^{\star}$_risk_percp_5 likely stems from the proximity to drivers and other passengers within the confined space of a taxi or ride-sharing vehicle.

Overall, the parameters are consistent with our theoretical expectations, providing a robust model that effectively captures the complexities of perceived risk during the COVID-19 pandemic.

5.2.3 Assessing the Impact of Perceived Risk on Scheduling Choices Working from Home and Working from Office

To demonstrate that risk perception impacts the scheduling of individuals, we combine the latent variable model with the choice model by using sequential estimation. Considering a binary choice model with two alternatives, where alternative 1 is Working From Home (WFH), and alternative 2 is Working From Office (WFO). For the sequential estimation, we use Eqs. (28) and (33), where the values of the coefficients $\beta_k^{\star}$ are the result of the estimation presented in Table 8. We have again a mixture of logit models, but with fewer parameters, as the parameters of the structural equation are not re-estimated. The estimated parameters of the choice model are presented in Table 6. The choice data we use from the survey is the categorical variable that gives the number of times an individual goes to the office per week during COVID-19, and we transform it into a binary variable. We pick this choice because it is the closest we can do to model the switching of activities given the risk perception. Specifically, an individual will choose 'home' as an activity instead of 'work' based on their perceived risk. If an individual works at least one time from home, we assign the choice as WFH instead of WFO.

	Value	**Rob. Std err**	**Rob. t-test**	**Rob. p-value**
ASC_{WFO}	0.754713	0.106462	7.089038	1.350475×10^{-12}
$\beta_{WFO}^{X^{\star}}$	1.828736	0.421655	4.337042	1.444132×10^{-5}
$\beta_{WFO}^{'T}$	-0.013845	0.003314	-4.177443	2.948044×10^{-5}
σ_s	0.387208	0.167638	2.309787	2.089995×10^{-2}

Table 6: Results of the choice model from the sequential estimation.

Interestingly, the parameter $\beta_{WFO}^{X^{\star}}$, associated with the latent variable of risk perception, is both positive and statistically significant. This indicates that an increased perception of risk correlates with a higher likelihood of individuals choosing to work from home rather than commute to the office. This finding underscores the impact of risk perception on activity-travel behavior and validates the inclusion of this latent variable model within the activity-based framework.[6]

However, due to the absence of actual choices and schedules of each individual throughout the day in the dataset, it is challenging to fully integrate the hybrid choice model

[6]The full estimation of the hybrid choice model, in which all the parameters are estimated simultaneously, can be found in the Appendix A, Table 9.

with the proposed ABRM. Consequently, our methodology is constrained by the need to make certain assumptions to integrate risk awareness in the previously proposed ABRM. Nonetheless, the latent variable of risk perception is statistically significant for the choice model of WFH vs WFO, underlining the fact that risk awareness is a non-negligible factor to consider in pandemic-oriented ABMs.

5.2.4 Integration of Risk in the ABRM: ABR^{2}M

Given the lack of data discussed in the previous section, to model the influence of the individual perceived risk due to COVID-19 on daily activity scheduling, we make the following assumption:

Hypothesis 1 *The perceived risk influences the ABM model by altering the desired duration of activities τ_{an} for every individual.*

That is to say: a higher perceived risk associated with an activity leads to a reduction in the time individuals are willing to allocate to that activity. This adaptive behavior is modeled by adjusting the desired activity durations τ_{an} from Equations (15) and (16), by using a sigmoid function with the mid-point set at υ_2, and a steepness of υ_1 [7]. The new desired duration becomes:

$$\tau'_{an} = \tau_{an} \frac{1}{1+\exp(-\upsilon_1(j^{\star}_{ni} - \upsilon_2))}, \tag{36}$$

where $j^{\star}_{ni}$, is the risk perceived by an individual n to perform an activity a from the indicators i associated to risk perception for that activity a. The algorithm to estimate of $j^{\star}_{ni}$ is discussed in the Appendix C, Algorithm 1. Through this mechanism, the updated ABRM model dynamically incorporates individual-level responses into the simulation of mobility and activity patterns.

5.2.5 Comparative schedules with or without latent variable model

We run the baseline scenario *'Normal Life'* with and without the latent variable model to assess the impact on how the perception of risk impacts the total count of individuals per type of activity. Figure 4a shows how, by accounting for the perception of risk in the secondary and work activities, we observe how people prefer to go very early in the morning to work but then stay home in the afternoon. Around lunchtime, the participation in secondary and work activities dramatically drops, reaching 80% and 50% reduction around lunchtime, respectively. The changes in the hourly count of individuals per activity, as shown in Figure 4b, highlight the greater sensitivity of work activities compared to secondary activities. The data indicates that individuals are more likely to avoid going to work during a pandemic, whereas they continue to engage in secondary activities. This

[7] Note that υ_1 and υ_2 need to be determined from data, and that we assume no mandatory participation in any activity. For this case study, the mid-point is set at 3 (which corresponds to 'Medium Risk'), and steepness of 1.5

phenomenon can be explained by the fact that many secondary activities, such as shopping, are essential and cannot be postponed, whereas work can often be conducted from home.

5.2.6 Discussion

Overall, these findings emphasize the impact of risk perception in shaping daily activity patterns. The alteration in schedules due to risk perception changes the frequency and timing of contacts in various facilities throughout the day. This shift influences the transmission dynamics of a disease, highlighting the importance of incorporating these behavioral changes into models. By doing so, we can better assess how different policies impact the number of infections, deaths, and the economic consequences of implementing restriction policies.

6 Conclusions

This study presents the Activity-Based Restriction & Risk aware Model (ABR^{2}M), which integrates individual risk perceptions and public health policies to simulate daily activity schedules during pandemics.

The model shows that activity restriction policies, such as curfews and closures, significantly alter daily activity patterns. Individuals adapt by rescheduling or substituting activities rather than eliminating them. For instance, the total duration of time spent at work by the population increases by 250% (in relative percentage) when all the activities are forbidden but work, highlighting the significant influence of activity swapping on daily routines when restrictions are applied. Perceived risk also modifies the timing and duration of activities, as individuals avoid high-risk activities. For example, the participation in secondary activities can drop by up to 80% around lunchtime, while work activities see a reduction of up to 50%. These behavioral changes are crucial for understanding shifts in mobility patterns and their impact on disease transmission.

The model is computationally robust, effectively handling large-scale populations and facility networks. It can generate approximately 7,000 schedules in one minute for an average city population, demonstrating significant speed compared to other models. However, it faces certain limitations. One major challenge is the availability of detailed data for calibrating risk perception. Additionally, the model simplifies transportation modes and excludes activity capacity constraints. To fully implement the model, we would need comprehensive datasets that include detailed schedules of individuals before and during a disease outbreak, their socioeconomic characteristics, and their attitudes towards the disease and activity participation.

Referring back to our research question: *"How do we account for risk perception and epidemic control restrictions in the context of mobility-based epidemiological models?"*,

this study has made significant progress in addressing this question by developing and validating the ABR^{2}M. The model incorporates both restriction policies and perceived risk, providing a more comprehensive understanding of how these factors influence daily activity schedules and, consequently, disease transmission dynamics.

Despite these advances, further work remains. Future research should focus on integrating the model into an epidemiological framework and proposing an optimal policy-making problem to contain future pandemics.

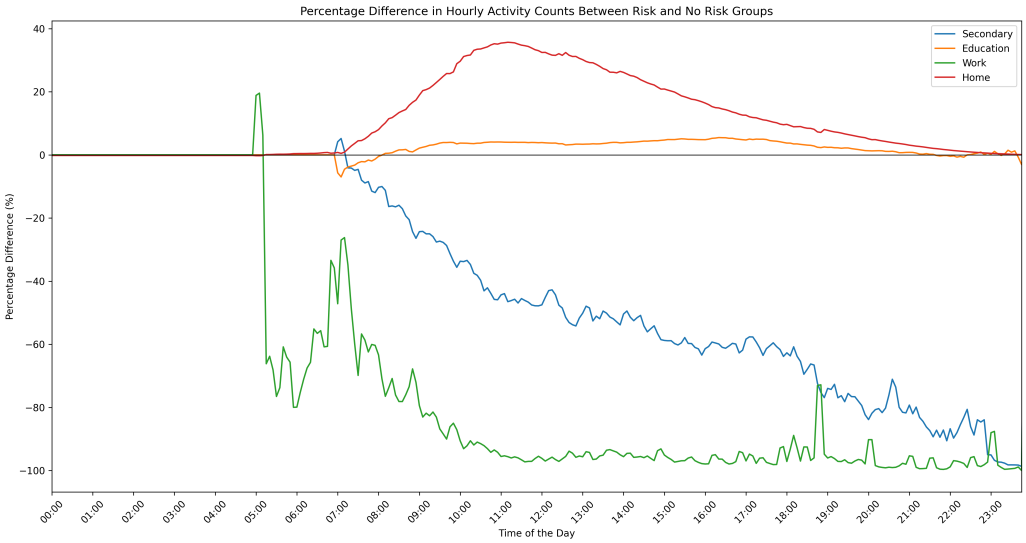

(a) Percentage difference in hourly activity counts between ABRM and ABR^{2}M

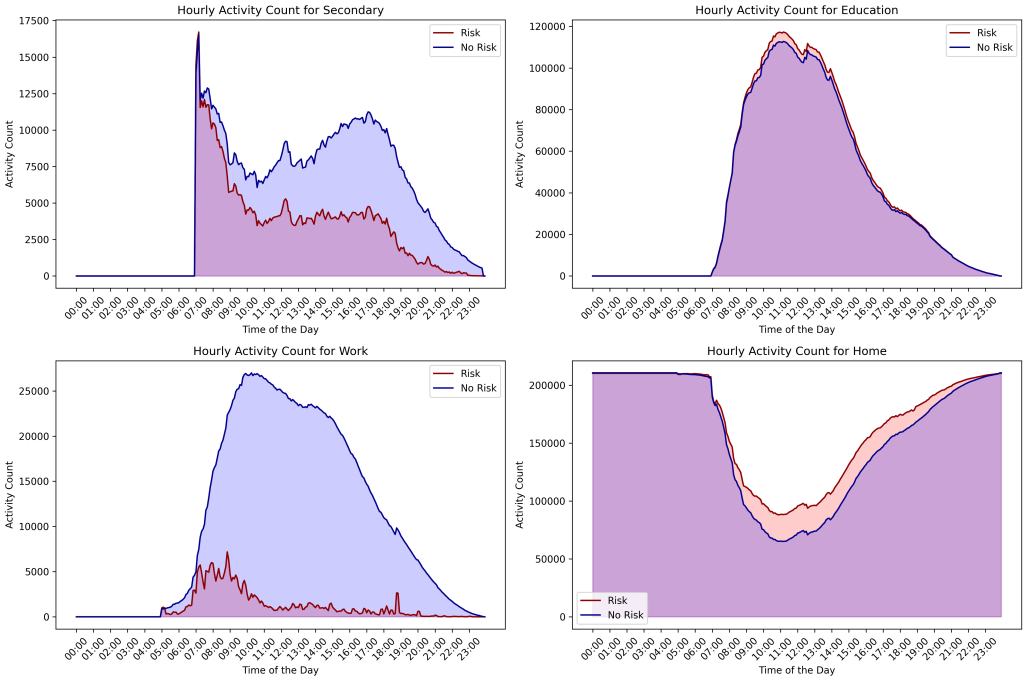

(b) Changes in hourly count of individuals per activity when between ABRM and ABR^{2}M.

Figure 4: Comparison of ABRM and ABR^{2}M results

References

Adler, T. and Ben-Akiva, M. (1979). A theoretical and empirical model of trip chaining behavior, Transportation Research Part B: Methodological **13**: 243–257.

Aleta, A., Martin-Corral, D., Pastore Y Piontti, A., Ajelli, M., Litvinova, M., Chinazzi, M., Dean, N. E., Halloran, M. E., Longini, I. M., Merler, S., Pentland, A., Vespignani, A., Moro, E. and Moreno, Y. (2020). Modelling the impact of testing, contact tracing and household quarantine on second waves of COVID-19, Nature Human Behaviour **4**(9): 964–971.

Alsharawy, A., Spoon, R., Smith, A. and Ball, S. (2021). Gender Differences in Fear and Risk Perception During the COVID-19 Pandemic, Frontiers in Psychology **12**: 689467.
URL: *https://www.frontiersin.org/articles/10.3389/fpsyg.2021.689467/full*

Arentze, T. and Timmermans, H. (2004). Albatross: A learning based transportation oriented simulation system, Transportation Research Part B: Methodological **38**: 613–633.

Beckman, R., Barrett, C., Berkbigler, K., Burris, K., Bush, B., Hull, S., Hurford, J., Medvick, P., Kubicek, D., Marathe, M., Morgeson, J., Nagel, K., Roberts, D., Smith, L., Stein, M., Stretz, P., Sydoriak, S., Cervenka, K. and Donnelly, R. (2002). Transportation analysis simulation system (transims) - the dallas-ft. worth case study.

Bowman, J. and Ben-Akiva, M. (2001). Activity-based disaggregate travel demand model system with activity schedules, Transportation Research Part A: Policy and Practice **35**: 1–28.

Charypar, D. and Nagel, K. (2005). Generating complete all-day activity plans with genetic algorithms, Transportation **32**: 369–397.

Chauhan, R. S., Bhagat-Conway, M. W., Magassy, T., Corcoran, N., Rahimi, E., Dirks, A., Pendyala, R., Mohammadian, A., Derrible, S. and Salon, D. (2022). COVID Future Panel Survey: A Unique Public Dataset Documenting How U.S. Residents' Travel Related Choices Changed During the COVID-19 Pandemic. arXiv:2208.12618 [cs, stat].
URL: *http://arxiv.org/abs/2208.12618*

Cortes Balcells, C., Krueger, R. and Bierlaire, M. (2023). Multi-objective Optimization of Activity-Travel Policies for Epidemic Control: Balancing Health and Economic Outcomes on Socio-Economic Segments.

Desaulniers, G., Desrosiers, J. and Solomon, M. M. (eds) (2005). Shortest Path Problems with Resource Constraints, GERAD 25th anniversary series, Springer, New York.

Hagerstrand, T. (2005). Reflections on 'what about people in regional science?', Papers in Regional Science - PAP REG SCI **66**: 1–6.

Hancean, M.-G., Slavinec, M. and Perc, M. (2021). The impact of human mobility networks on the global spread of COVID-19, Journal of Complex Networks **8**(6): cnaa041.
URL: *https://academic.oup.com/comnet/article/doi/10.1093/comnet/cnaa041/6161495*

He, B. Y., Zhou, J., Ma, Z., Chow, J. Y. and Ozbay, K. (2020). Evaluation of city-scale built environment policies in New York City with an emerging-mobility-accessible synthetic population, Transportation Research Part A: Policy and Practice **141**: 444–467.
URL: *https://linkinghub.elsevier.com/retrieve/pii/S096585642030745X*

Kerr, C. C., Stuart, R. M., Mistry, D., Abeysuriya, R. G., Hart, G., Rosenfeld, K., Selvaraj, P., Nunez, R. C., Hagedorn, B., George, L., Izzo, A., Palmer, A., Delport, D., Bennette, C., Wagner, B., Chang, S., Cohen, J. A., Panovska Griffiths, J., Jastrzebski, M., Oron, A. P., Wenger, E., Famulare, M. and Klein, D. J. (2020). Covasim: an agent-based model of COVID-19 dynamics and interventions. Pages: 2020.05.10.20097469.
URL: *https://www.medrxiv.org/content/10.1101/2020.05.10.20097469v1*

Lu, H., Yang, J., Zhao, K., Jin, Z., Wen, X., Hu, N., Yang, H., Sun, Z., Chen, H., Huang, Y., Wang, D. B. and Wu, Y. (2024). Perceived risk of COVID-19 hurts mental health: the mediating role of fear of COVID-19 and the moderating role of resilience, BMC Psychiatry **24**(1): 58.
URL: *https://bmcpsychiatry.biomedcentral.com/articles/10.1186/s12888-024-05511-x*

Mazzoli, M., Mateo, D., Hernando, A., Meloni, S. and Ramasco, J. J. (2020). Effects of mobility and multi-seeding on the propagation of the COVID-19 in Spain, preprint, Epidemiology.
URL: *http://medrxiv.org/lookup/doi/10.1101/2020.05.09.20096339*

Palguta, J., Levinsky, R. and Skoda, S. (2022). Do elections accelerate the COVID-19 pandemic?: Evidence from a natural experiment, Journal of Population Economics **35**(1): 197–240.
URL: *https://link.springer.com/10.1007/s00148-021-00870-1*

Pougala, J., Hillel, T. and Bierlaire, M. (2022). Capturing trade-offs between daily scheduling choices, Journal of Choice Modelling **43**: 100354.
URL: *https://linkinghub.elsevier.com/retrieve/pii/S1755534522000124*

Recker, W., McNally, M. and Root, G. (1986). A model of complex travel behavior: Part i theoretical development, Transportation Research Part A: General **20**(4): 307–318.
URL: *https://www.sciencedirect.com/science/article/pii/0191260786900890*

Rosi, A., Van Vugt, F. T., Lecce, S., Ceccato, I., Vallarino, M., Rapisarda, F., Vecchi, T. and Cavallini, E. (2021). Risk Perception in a RealWorld Situation (COVID19):

How It Changes From 18 to 87 Years Old, Frontiers in Psychology **12**: 646558.
URL: *https://www.frontiersin.org/articles/10.3389/fpsyg.2021.646558/full*

Torres, F., Gendreau, M. and Rei, W. (2022a). Crowdshipping: An open VRP variant with stochastic destinations, Transportation Research Part C: Emerging Technologies **140**: 103677. Publisher: Elsevier.
URL: *https://www.sciencedirect.com/science/article/pii/S0968090X22001188*

Torres, F., Gendreau, M. and Rei, W. (2022b). Vehicle Routing with Stochastic Supply of Crowd Vehicles and Time Windows, Transportation Science **56**(3): 631–653.
URL: *https://pubsonline.informs.org/doi/10.1287/trsc.2021.1101*

Tuomisto, J. T., Yrjola, J., Kolehmainen, M., Bonsdorff, J., Pekkanen, J. and Tikkanen, T. (2020). An agent-based epidemic model REINA for COVID-19 to identify destructive policies, preprint, Infectious Diseases (except HIV/AIDS).
URL: *http://medrxiv.org/lookup/doi/10.1101/2020.04.09.20047498*

A Additional Data and Tables

Variable Name	Description	Type	Counts
age_above_60	Is the individual above 60 years old?	Binary	578
age_bw_30_60	Is the individual between 30 and 60 years old?	Binary	2259
age_under_30	Is the individual under 30 years old?	Binary	553
gender_female	Is the individual female?	Binary	2057
notCaucasian	Is the individual not Caucasian?	Binary	684
bachelors_or_more	Does the individual have a bachelor's degree or more?	Binary	2059
technical_school	Did the individual attend technical school?	Binary	918
high_school	Did the individual graduate from high school?	Binary	413
worker	Is the individual currently employed?	Binary	3390
zone_Midwest	Is the individual located in the Midwest zone?	Binary	779
zone_Northeast	Is the individual located in the Northeast zone?	Binary	404
zone_South	Is the individual located in the South zone?	Binary	974
zone_West	Is the individual located in the West zone?	Binary	1229
income_below_35	Is the individual's income below $35k?	Binary	545
income_35_to_100	Is the individual's income between $35k and $100k?	Binary	1495
income_above_100	Is the individual's income above $100k?	Binary	1350
hh_single	Is the household single?	Binary	534
hh_partner	Is the household in partnership?	Binary	2046
hh_children	Does the household have children?	Binary	1182
hh_parents	Does the household have parents?	Binary	389
single_only	Is the individual single only in the household?	Binary	534
partner_only	Is the individual in partnership only in the household?	Binary	1110
children_only	Is the individual responsible for children only in the household?	Binary	216
parents_only	Is the individual responsible for parents only in the household?	Binary	238
partner_and_children	Is the individual in partnership and responsible for children in the household?	Binary	851
partner_and_parents	Is the individual in partnership and responsible for parents in the household?	Binary	36
children_and_parents	Is the individual responsible for both children and parents in the household?	Binary	66
multiple_automobiles	Does the household own multiple automobiles?	Binary	2119
hhsize_1	Is the household size 1?	Binary	565
hhsize_2	Is the household size 2?	Binary	1125
hhsize_3	Is the household size 3?	Binary	665
hhsize_4	Is the household size 4?	Binary	616
hhsize_4plus	Is the household size more than 4?	Binary	419
hhfamilyhouse	Is the household a family house?	Binary	2616
hhapartment	Is the household an apartment?	Binary	655
hhnonstandard	Is the household a nonstandard housing type?	Binary	119
hhyard	Does the household have a yard?	Binary	2877
covid_positive	Is the individual COVID-19 positive?	Binary	154

Table 7: Explanatory variables for the Latent Model

Name	Value	Rob. Std err	Rob. t-test	Rob. p-value
$\alpha^\star$_att_covid_friendssevere	0.416	0.107	3.87	1.08×10^{-4}
$\alpha^\star$_att_covid_stayhome	0.753	0.111	6.79	1.12×10^{-11}
$\alpha^\star$_att_covid_sh_norm	0.523	0.123	4.25	2.13×10^{-5}
$\alpha^\star$_risk_percp_1	0.64	0.127	5.04	4.54×10^{-7}
$\alpha^\star$_risk_percp_2	0.376	0.0878	4.28	1.86×10^{-5}
$\alpha^\star$_risk_percp_3	0.372	0.0874	4.26	2.08×10^{-5}
$\alpha^\star$_risk_percp_5	0.273	0.0792	3.45	5.62×10^{-4}
$\alpha^\star$_risk_percp_6	0.406	0.0891	4.55	5.27×10^{-6}
$\alpha_0^\star$_att_covid_friendssevere	-0.539	0.0309	-17.4	0
$\alpha_0^\star$_att_covid_stayhome	-0.489	0.0333	-14.7	0
$\alpha_0^\star$_att_covid_sh_norm	0.0953	0.0332	2.87	4.07×10^{-3}
$\alpha_0^\star$_risk_percp_1	0.0959	0.0347	2.76	5.73×10^{-3}
$\alpha_0^\star$_risk_percp_2	0.0615	0.0229	2.68	7.4×10^{-3}
$\alpha_0^\star$_risk_percp_3	-0.51	0.026	-19.6	0
$\alpha_0^\star$_risk_percp_5	-0.127	0.0219	-5.78	7.27×10^{-9}
$\alpha_0^\star$_risk_percp_6	-0.493	0.027	-18.2	0
$\sigma^\star$_att_covid_friendssevere	0.778	0.0226	34.5	0
$\sigma^\star$_att_covid_stayhome	0.924	0.0242	38.1	0
$\sigma^\star$_att_covid_sh_norm	0.766	0.0195	39.3	0
$\sigma^\star$_risk_percp_1	0.72	0.0189	38	0
$\sigma^\star$_risk_percp_2	0.492	0.0127	38.7	0
$\sigma^\star$_risk_percp_3	0.62	0.0185	33.5	0
$\sigma^\star$_risk_percp_5	0.547	0.0141	38.7	0
$\sigma^\star$_risk_percp_6	0.643	0.0184	35	0
$\beta^\star$_gender_female	-0.25	0.0478	-5.23	1.67×10^{-7}
$\beta^\star$_intercept	-0.103	0.0388	-2.66	7.83×10^{-3}
$\beta^\star$_notCaucasian	-0.265	0.0509	-5.2	1.94×10^{-7}
$\beta^\star$_technical_school	0.142	0.0583	2.44	1.47×10^{-2}
$\beta^\star$_zone_West	0.0905	0.0421	2.15	3.16×10^{-2}
δ_1	0.266	0.0063	42.2	0
δ_2	0.581	0.0129	45	0

Table 8: Results parameters Latent model

Name	Value	Rob. Std err	Rob. t-test	Rob. p-value
ASC_WFO	0.635	0.0846	7.51	5.86×10^{-14}
$\beta^{X^\star}_{WFO}$	1.92	0.497	3.87	1.11×10^{-4}
$\beta^{'T}_{WFO}$	-0.0138	0.00338	-4.09	4.25×10^{-5}
$\alpha^\star$_att_covid_friendssevere	0.403	0.0862	4.68	2.94×10^{-6}
$\alpha^\star$_att_covid_selfsevere	0.382	0.0972	3.92	8.68×10^{-5}
$\alpha^\star$_att_covid_stayhome	0.701	0.0939	7.47	8.15×10^{-14}
$\alpha^\star$_att_covid_sh_norm	0.508	0.104	4.9	9.62×10^{-7}
$\alpha^\star$_risk_percp_1	0.537	0.105	5.13	2.96×10^{-7}
$\alpha^\star$_risk_percp_2	0.259	0.0746	3.47	5.19×10^{-4}
$\alpha^\star$_risk_percp_3	0.25	0.076	3.29	1.00×10^{-3}
$\alpha^\star$_risk_percp_5	0.208	0.0676	3.08	2.08×10^{-3}
$\alpha^\star$_risk_percp_6	0.348	0.0796	4.37	1.22×10^{-5}
$\alpha^\star_0$_att_covid_friendssevere	-0.532	0.029	-18.3	0
$\alpha^\star_0$_att_covid_selfsevere	-0.188	0.0306	-6.12	9.09×10^{-10}
$\alpha^\star_0$_att_covid_stayhome	-0.494	0.032	-15.5	0
$\alpha^\star_0$_att_covid_sh_norm	0.0876	0.0323	2.71	6.67×10^{-3}
$\alpha^\star_0$_risk_percp_1	0.0795	0.0328	2.42	1.54×10^{-2}
$\alpha^\star_0$_risk_percp_2	0.0492	0.0223	2.21	2.71×10^{-2}
$\alpha^\star_0$_risk_percp_3	-0.503	0.0257	-19.5	0
$\alpha^\star_0$_risk_percp_5	-0.124	0.0217	-5.71	1.13×10^{-8}
$\alpha^\star_0$_risk_percp_6	-0.489	0.027	-18.1	0
$\sigma^\star$_att_covid_friendssevere	0.761	0.0209	36.4	0
$\sigma^\star$_att_covid_selfsevere	0.845	0.0204	41.5	0
$\sigma^\star$_att_covid_stayhome	0.916	0.0229	40	0
$\sigma^\star$_att_covid_sh_norm	0.755	0.0181	41.8	0
$\sigma^\star$_risk_percp_1	0.708	0.0175	40.4	0
$\sigma^\star$_risk_percp_2	0.487	0.0119	40.8	0
$\sigma^\star$_risk_percp_3	0.621	0.0171	36.3	0
$\sigma^\star$_risk_percp_5	0.542	0.0133	40.9	0
$\sigma^\star$_risk_percp_6	0.643	0.0173	37.1	0
$\beta^\star$_gender_female	-0.251	0.044	-5.69	1.27×10^{-8}
$\beta^\star$_intercept	-0.177	0.0409	-4.33	1.47×10^{-5}
$\beta^\star$_notCaucasian	-0.216	0.0523	-4.13	3.69×10^{-5}
$\beta^\star$_technical_school	0.24	0.0622	3.86	1.11×10^{-4}
$\beta^\star$_zone_West	0.1	0.0415	2.42	1.56×10^{-2}
δ_1	0.257	0.00573	44.9	0
δ_2	0.592	0.0124	47.8	0

Table 9: Results parameters of the hybrid choice model.

Notation	Description
Z_a^0	binary variable set to 1 if activity a is scheduled during the day, 0 otherwise
Z_b^0	binary variable set to 1 if activity b is scheduled during the day, 0 otherwise
Z_{ab}	binary variable set to 1 if activity b follows immediately activity a where $a \neq b$
x_a^1	discrete variable representing the starting time of activity a
x_b^1	discrete variable representing the starting time of activity b
x_a^2	discrete variable representing the duration of activity a
ω_{dawn}	discrete variable representing the starting time of the activity at dusk time
ω_{dusk}	discrete variable representing the starting time of the activity at dusk time
κ_a	discrete parameter representing the desired starting time of activity a
τ_a	discrete parameter representing the desired duration of activity a
ω_{ab}	discrete parameter representing the travel time between facilities a and b
Δ_a	discrete parameter representing the flexibility level of activity a
χ_a	utility associated with participating in an activity during day a
θ_t	travel time penalty
θ_a	penalty for activity a for starting early, late, being short, or being long
t_Θ^1	user-defined time slot to start an activity
t_Θ^2	user-defined time slot to end an activity
t_Θ^3	user-defined start closing time to avoid peak hours
t_Θ^4	user-defined end closing time to avoid peak hours
t_Θ^5	user-defined maximum travel time
t_Θ^6	user-defined staying at home time
t_Θ^7	user-defined starting time of dusk activities
t_Θ^8	user-defined maximum allowed time in an activity

Table 10: Description of the variables and parameters

B Dynamic Programming Algorithm

Dominance rules have to be developed carefully so that we can delete the highest number of labels and guaranty that the optimal solution is not deleted from the list of labels.

B.1 Dominance Rules

Label $\mathscr{L}_1$ dominates label $\mathscr{L}_2$ if the following rules are true:

1. $a_1 = a_2$
2. $t_1 = t_2$
3. $x_1 = x_2$
4. $U_1 - u_1 > U_2 - u_2$
5. $\mathscr{R}_1 \subseteq \mathscr{R}_2$

Lemma 1 All future activity schedules reachable from a label $\mathscr{L}_1$, dominated by another label $\mathscr{L}_2$ using the dominance rules are reachable from label $\mathscr{L}_2$ with higher cumulative utility.

Proof Notice that the current activity and time for both labels are the same, i.e., $a_1 = a_2$ and $t_1 = t_2$. Also the time, cost, and resource consumption for each extension is the same for all combination of activities. Hence, time constraints or any resource constraint cannot be violated for any future sequence of activities for label $\mathscr{L}_1$ but not for label $\mathscr{L}_2$, i.e., if the extension is not feasible to $\mathscr{L}_1$ then certainly it will not be feasible for $\mathscr{L}_2$. Now, utility will be the same for all extensions due to the dominance (2) and due to dominance rule (4) the previous utility must be strictly lower for the dominated label.

The result can be more formally arrived to by contradiction. We suppose it was not true, i.e., that some resource will be higher, and then arrive to a contradicting result.

By Lemma 1, we can prove that all future extensions are possible without worsening the value of the objective function. Even though, the utility is a function that depends on the start time, and duration of the activity.

Proposition The Dominance rules do not eliminate the optimal solution if a solution exists.

Proof Let $\mathscr{L}_i$ be a dominated label by a label $\mathscr{L}_j$ and let $P^i = \{a_1, \ldots, a_i\}$ be the sequence of activities performed by label $\mathscr{L}_i$, similarly, let $P^j = \{a_1, \ldots, a_j\}$ be the sequence of activities performed by label $\mathscr{L}_j$, and let $a_1 =$ home, i.e., the start of the schedule.

By contradiction, suppose that an optimal solution does exist with path $P^* = \{a_1, \ldots, a_i, \ldots a_1\}$, i.e., a path obtained from an extension of the dominated label with a total optimal utility of U^*. However, we can create a new path by replacing the dominated

label with label $\mathscr{L}_j$, i.e., $P^z = \{a_1, \ldots, a_j, \ldots a_1\}$ with a total utility of U^z. By Lemma 1 we know that $U^z > U^*$ hence contradicting the assumption that P^* is optimal.

B.2 Decremental State Space Relaxations (DSSR)

Decremental State Space Relaxations (DSSR) are procedures applied to dynamicy programming where we relax the state space and gradually decrease the relaxation if the solution violates the constraints. In our case, the complicated constraints are the elementarity constraints, (i.e., that an activity can only be done once). Hence, dominance rule 5 (i.e., $\mathscr{R}_1 \subseteq \mathscr{R}_2$) is dropped. However, the solution to the relaxation can be infeasible since an activity can be performed several times in the relaxed problem. With DSSR we add a dominance rule 5 just for the repeated activity in the best solution found and not in every activity. In this way, the relaxation is decreased gradually, and the number of labels does not increase as rapidly.

Algorithm 1: Basic DP

```
Initiate time, t ← 0;
Initiate the list of labels, Label[1] = {ℒ_0 = (home, 0, 1, 1, 0, 0, {})};
while t ≠ 𝒯 do
    t ← t + 1;
    for ℓ_1 in Label[t] do
        Extend label to all feasible extensions;
        ℒ* ← feasible extension;
        t* ← REF(t);
        for ℓ_2 in Label[t*] do
            Apply dominance rules;
            if ℓ_2 is dominated then
                delete ℓ_2;
                continue;
            if ℒ* is dominated then
                delete ℒ*;
                break;
        Label[t*] ∪ ℒ*
return Best label at time 𝒯
```

B.3 DP heuristic

The dynamic programming algorithm introduced previously is exact (1), i.e., it finds the optimal solution. In practice, the population of individuals in a region can be over millions, thus, a fast solution is required to apply the algorithm to a large population. A heuristic method was developed that is faster than the exact DP algorithm by simple modifying the dominance rules. The dominance rule 3 was removed, while maintaining the

feasibility checks. Feasibility checks ensures that the solution will be feasible, while by relaxing rule 3 allows us to delete more labels. As a consequence, we lose the guaranty of finding an optimal solution, but we get fast solutions, necessary to analyze large populations.

C Algorithms

Algorithm 2: Draw from X_n^*, Compute Probabilities, and Assign the Maximum Probability Category for Each Individual and Risk Perception Indicator

Input: $\beta_0^*, \beta_k^*, \alpha_{0i}^*, \alpha_i^*, \sigma_i^*, \tau_j, x_{kn}^*, N, J, I, \text{num\_draws} = 1000$
Output: Assigned category value $j^\star$ for each individual n and indicator i
for each indicator $i = \text{risk\_percp\_m}$ for $m = 1, \cdots, 6$ **do**
  for each individual $n = 1$ to N **do**
    Initialize an empty list p_{sum} of length J with zeros;
    for each draw $d = 1$ to num_draws **do**
      Draw $\epsilon^* \sim \mathcal{N}(0,1)$;
      $X_n^* \leftarrow \beta_0^* + \sum_{k=1}^{K} \beta_k^* x_{kn}^* + \sigma_i^* \epsilon^*$;
      for each category $j = 1$ to J **do**
        if $j = 1$ **then**
          $p_j \leftarrow \Phi\left(\frac{\tau_j - \alpha_{0i}^* - \alpha_i^* X_n^*}{\sigma_i^*}\right)$;
        else
          $p_j \leftarrow \Phi\left(\frac{\tau_j - \alpha_{0i}^* - \alpha_i^* X_n^*}{\sigma_i^*}\right) - \Phi\left(\frac{\tau_{j-1} - \alpha_{0i}^* - \alpha_i^* X_n^*}{\sigma_i^*}\right)$;
        $p_{sum}[j] \leftarrow p_{sum}[j] + p_j$;
    $j^\star \leftarrow \arg\max_j p_{sum}[j]$;
    Store $j^\star$ for individual n and indicator i;